ORGANIC PROCESS RESEARCH & DEVELOPMENT
OPR&D

Open Access
This article is licensed under CC-BY-NC-ND 4.0

pubs.acs.org/OPRD
Article

Can Ultrasound Replace Seeding in Flow Reactive Crystallization of an Aromatic Amine?

Biyu Zhang, Georgios D. Stefanidis, and Tom Van Gerven*

Cite This: https://doi.org/10.1021/acs.oprd.4c00385
Read Online

ACCESS | Metrics & More | Article Recommendations | Supporting Information

ABSTRACT: Continuous crystallization has gained substantial interest due to its high product reproducibility, high labor efficiency, and low capital and production costs. Continuous seeding is preferable and often even required in the application of pharmaceuticals, which presents a bottleneck in continuous crystallization. This work proposes to apply ultrasound for continuous in situ seeding in the continuous reactive crystallization of an aromatic amine. Flow crystallization experiments with both ultrasound and conventionally prepared seeds were conducted. It was found that sonication initiated nucleation and continuously produced crystals in a stable manner. The nucleation rate could be controlled by adjusting the sonication power, highlighting the advantages of the sonicated seed generation strategy. Experiments under different flow conditions demonstrated that a higher flow rate combined with an appropriate sonication power was favorable for robust particle quality, reduced likelihood of clogging, and better reproducibility. Compared with the conventional addition of seed crystals, sonication-induced crystallization achieved higher yields and produced products with a narrow and unimodal size distribution. All sonicated experiments exhibited high robustness, indicating the feasibility and reliability of this method as a replacement for conventional seeding techniques in the continuous reactive crystallization of the studied compound. In summary, using ultrasound for continuous in situ seeding of the aromatic amine offers unique advantages in process robustness and product quality control, providing a promising strategy for continuous crystallization of similar systems.

KEYWORDS: *ultrasound, continuous crystallization, reactive crystallization, seeding, particle size, size distribution*

Downloaded via TU DORTMUND on December 11, 2024 at 08:55:09 (UTC).
See https://pubs.acs.org/sharingguidelines for options on how to legitimately share published articles.

1. INTRODUCTION

Crystallization is one of the most important separation and purification methods in the industry of various materials such as food, fine chemicals, active pharmaceutical ingredients (APIs), and proteins.[1,2] Although batch production still predominates in the crystallization industry, the continuous crystallization process especially in the manufacturing of pharmaceuticals has gained increasing attention in scientific research due to the benefits of high reproducibility, high scalability, and low capital and production costs.[3−6] For example, Eren et al.[7] reviewed the use of a mixed suspension mixed product removal (MSMPR) crystallizer in continuous API manufacture from the aspects of modeling and process design and the application of process analytical technology (PAT); Pu et al.[8] discussed the recent progress of continuous protein crystallization in both MSMPR crystallizer and tubular crystallizers; and Orehek et al.[9] presented the transition of the API crystallization process from batch to continuous system and the implementation of continuous crystallization in fully continuous upstream and downstream processes. There are many other review papers on the development of continuous crystallization, including the application of PAT tools,[10] different crystallizer configurations,[11] the design of lab-scale continuous crystallization system involving the seeding strategies,[12] the understanding of the impurity inclusion mechanism and control of impurities,[13] the common scaling/encrustation problem in the continuous crystallization processes,[14] etc., which the interested reader can consult further.

Using seeds in continuous crystallization is very common due to its benefits in controlling the particle size distribution,[15] producing the desired polymorphic crystals,[16,17] and reducing clogging.[18] Traditionally, the seed suspension is prepared and treated in advance (e.g., sieving[19,20] or ultrasonic comminution[21,22]), and then pumped into the continuous crystallizers. There are some application instances of this style of seeding in the cooling crystallization systems,[17,19,20] antisolvent crystallization systems,[23] and protein crystallization.[24] However, the operation duration of the continuous crystallization process could be limited to the quantity of seed crystals fed by this offline seeding technique[19,25] and the potential sedimentation of seeds on the wall of tubing.[26] Another consideration is that the product quality is highly dependent on the seeding conditions such as seed loading, seed size, and the seed addition methods,[12,15,27,28] which results in high requirements for the seed material preparation and, thus, a high time investment.[29,30] Moreover, the addition of seed crystals may bring impurities to the crystallization system and this kind of

Received: September 11, 2024
Revised: November 19, 2024
Accepted: November 22, 2024

© XXXX The Authors. Published by American Chemical Society

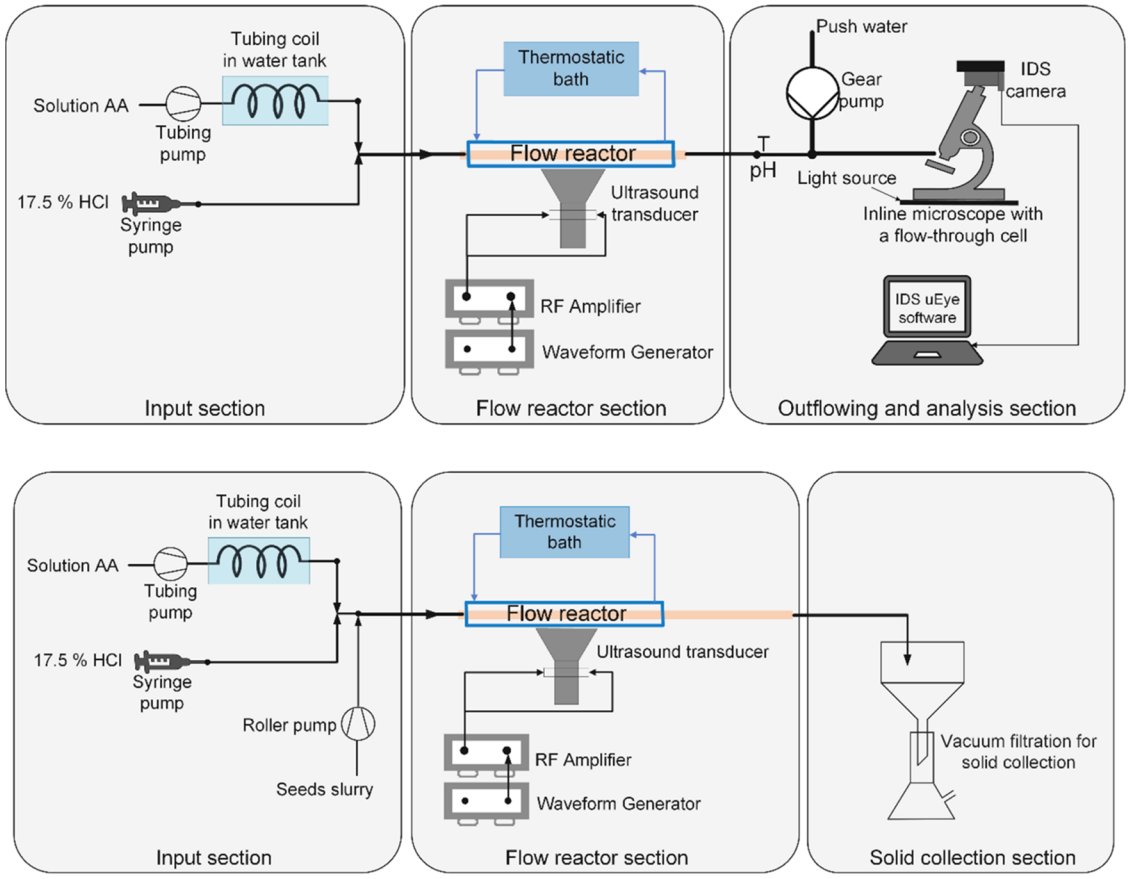

Figure 1. Schematic diagram of flow setup: reactor connecting to an inline microscope (top), modified reactor (extended length, having 3 times the volume), including a solid collection section (bottom).

process contamination should be avoided particularly in the pharmaceutical industry.[29] Therefore, an improved seeding technique that does not require additional seed materials would be preferable in the continuous crystallization process.

A continuous in situ seed generation instead of seed addition could be beneficial to the optimization of product quality and the improvement of process efficiency and robustness in the development of a continuous crystallization process. There are relatively few papers reporting this continuous seeding strategy. Jiang et al.[31] employed a dual-impinging-jet mixer[32,33] to continuously produce seed crystals in the semicontinuous crystallization of L-asparagine. Wu et al.[34] integrated a single-stage MSMPR crystallizer for in situ seed generation with a continuous oscillatory baffled crystallizer (COBC) for crystallization of ortho-aminobenzoic acid, by which combination it could be able to control the crystal size distribution and polymorphic form. Similarly, Gao et al.[16] designed an MSMPR-Tubular crystallizer system for a continuous supply of seeds in the continuous crystallization of α-form L-glutamic acid. Qamar et al.[35] investigated different seeding and operating strategies by modeling and simulation which included continuous seeding and periodic seeding combined or not with continuous fines removal.

Except for using micromixers and single-stage MSMPR, another in situ seed generation approach is ultrasonication, which is not new to the crystallization field. Good overviews of sonocrystallization technologies are given in refs 36−40. For the continuous crystallization process, many benefits of ultrasound have been reported such as anticlogging,[41,42] polymorphic control,[43−45] induction time reduction,[45,46] and particle size control.[46−49] Several papers have reported combining cooling with sonication for continuous seed generation. In the cooling crystallization of acetylsalicylic acid studied by Eder et al.,[50] continuous seed generation was achieved simply by immersing a separate feed tube into a cooling and ultrasonic bath, resulting in constant seed quantity and quality. Schmalenberg et al. applied a similar ultrasonic unit, which was built up from a CFI-designed tube (coiled flow inverter) immersed in an ultrasonic bath,[51] and further combined it with a CFI crystallizer[52] for cooling crystallization of amino acids. Jiang et al.[53] employed an ultrasonication probe to press against a tube to achieve continuous nucleation, and further integrated it into a slug-flow crystallizer for continuous cooling crystallization of L-asparagine. They found that ultrasound-assisted seeding strategy could produce more uniform-sized seed crystals and less likely to clog than using micromixers.[54] Another advantage is that sonication can give a controllable nucleation rate reported by Jiang et al.[53] and Vancleef et al.[55,56] Using sonication for continuous in situ seeding has many application instances in continuous cooling crystallization systems, while reports on the applications in other crystallization systems are relatively limited.

In the present work, the application of ultrasound in the continuous reactive crystallization of an Aromatic Amine (written as AA below) was investigated from the perspective of seeding. Ultrasound can help particle size control without changing the crystal form, which was known from the earlier study on batch reactive crystallization of AA.[57] The question

https://doi.org/10.1021/acs.oprd.4c00385
Org. Process Res. Dev. XXXX, XXX, XXX−XXX

Table 1. Nucleation Experiments under Both Silent and Sonicated Conditions

ultrasound frequency (kHz)	ultrasound amplitude (mVpp)	electrical power (W)	solution AA flow rate (mL/min)	solution HCl Flow rate (mL/min)	residence time in reactor (s)	push water flow rate (mL/min)	traveling time in tubes (s)[a]
42.8	0	0[b]	3	0.21	47	10	4.8
			6	0.42	23.5	10	2.9
	80	2	3	0.21	47	10	4.8
			6	0.42	23.5	10	2.9
	130	5	3	0.21	47	10	4.8
			6	0.42	23.5	10	2.9
	180	8	3	0.21	47	10	4.8
			6	0.42	23.5	10	2.9
	220	11	3	0.21	47	10	4.8
			6	0.42	23.5	10	2.9

[a]Traveling time corresponds to the residence time in the tube between the outlet of the reactor and the flow-through cell. [b]Silent conditions correspond to the case of 0 W of electrical power. For each sonication power, two flow conditions were conducted. Each condition was repeated three times.

Table 2. Unseeded and Sonicated Crystallization Experiments, Involving Solid Collection[a]

ultrasound frequency (kHz)	ultrasound amplitude (mVpp)	electrical power (W)	volume of reactor (mL)	AA flow rate (mL/min)	HCl flow rate (mL/min)	residence time in sonicated volume (s)	residence time in sonication-free volume (s)	total residence time (s)	total collection time (s)
42.8	180	8	2.5	3	0.21	47.0	0.0	47.0	240
				6	0.42	23.5	0.0	23.5	
				12	0.84	11.7	0.0	11.7	
			7.5	3	0.21	47.0	93.9	140.9	
				6	0.42	23.5	47.0	70.5	
				12	0.84	11.7	23.5	35.2	

[a]Same sonication condition, in two reactors with different volumes. Three flow conditions were conducted. Each condition was repeated three times.

raised here is whether ultrasound can be used in the continuous process to replace the conventional seeding method. Focusing on that, flow reactive crystallization experiments of AA were designed with and without ultrasound and further compared with the conventional seeded experiments. Different flow conditions were tested, together with the analysis of nucleation and final particle properties, to give a comprehensive evaluation of sonication versus conventional seeding in the continuous manufacturing of AA. This research contributes to addressing the existing gap in continuous in situ seed generation methods and provides a guideline for the application of ultrasound in continuous reactive crystallization systems.

2. MATERIALS AND METHODS

2.1. Chemicals. There are two reactant solutions in the studied flow crystallization system: solution of aromatic amine and HCl. Solution AA was prepared as the desired concentration by the industrial partner, involving compound AA (25% w/v actual; 99%, industrially provided), sodium acetate (20% w/v actual; Anhydrous, Reagent-plus, Merck Life Science), ultrapure water (50% w/v actual; 18.2 MΩ·cm), and methanol (25% w/v actual; 99.9% purity, Merck Life Science). Sodium acetate from upstream in the industrial process takes up the role of noncrystallizing cosolute in this system, as proven in batch crystallization experiments (available in Data S1). NaOH (50 wt %, solution for analysis, Merck Life Science) of 1.3 mol equiv with respect to compound AA was added to dissolve the compound and get an anionic solution. HCl (17.5 wt %, diluted from HCl of 37%, Merck Life Science) as the other reactant was used to neutralize the anionic solution AA and further obtain the protonated crystals. The chemical reaction is a neutralization reaction of the basic sodium salt solution with HCl, following $AA^- + H^+ \rightarrow AA\ (L) \rightarrow AA\ (S)$, similar to the precipitation of L-glutamic acid by mixing sodium L-glutamate and sulfuric acid.[58]

Slurry AA for seeded experiments was prepared by adding excessive compound AA into the binary solvent of water and methanol (weight ratio 2:1) and stirring for 24 h. The solid content was determined by weight method as 2.8% w/v. This solid content is reasonable from the perspective of injecting seeds, neither too thin (giving sufficient seeds without introducing too much solvent) nor too dense (a controllable flow rate via a peristaltic pump). The flow conditions of seed slurry are given in Section 2.3.

Acetonitrile (99.9% purity, Merck Life) was used as the dispersant during the measurements of the particle size distribution (PSD).

2.2. Flow Setup Design. Figure 1 shows a schematic diagram of the setup. The flow setup consists of three parts. The main body of the setup is a glass tube crystallizer (inner diameter 4 mm, length 20 cm, volume 2.5 mL) with an outside rectangular jacket connecting to the thermostatic bath (Julabo HE Lab thermostat). A plate ultrasound transducer (Ultrasonics World MPI-7850D-20_40_60H, diameter 7.8 cm) is attached to the bottom of the jacket to sonicate the crystallizer. A waveform generator (Picotest G5100A) and an amplifier (E&I 1020L RF power amplifier) are used to set the ultrasound frequency and amplitude, respectively. Tables 1 and 2 list the frequency and amplitude data applied in this study.

https://doi.org/10.1021/acs.oprd.4c00385
Org. Process Res. Dev. XXXX, XXX, XXX−XXX

The second part is the input section of the two reactants. Reactant solution HCl is pumped using a Chemyx Fusion 4000 syringe pump, capable of flow rates from 0.0001 to 170.5 mL/min, depending on the syringe used. For this process, a 50 mL Terumo syringe is used, providing a flow rate range of 9.3527 μL/h to 118.52 mL/min. Reactant Solution AA is pumped by an Ismatec tubing pump (Ismatec Reglo Digital, MS-4/08-100, flow rate 0.002−35 mL/min). It flows through a tubing coil placed in a water tank to reach the desired temperature of 25 ± 3 °C. The effects of the slight temperature difference at around 25 °C on this reactive crystallization system are ignored. The temperature change during sonication is tracked by the type-K thermocouples connected to a Pico TC-08 data logger. The thermocouples are only for testing the thermal retention of the water tank and the housing jacket; afterward, they are removed to avoid scaling problems. An example of the temperature profile can be found in Data S2. A pH meter (Mettler Toledo Transmitter M300 with a pH Sensor InPro4260i) is used to manually measure the pH of the outflowing slurry.

The third part is the outflowing section. An inline microscope based on the flow-through microscopy in the work of Vancleef et al.[59] is used to analyze the nucleation process quantitatively. A stereomicroscope (Nikon, SMZ800N, defined magnification of 40×) equipped with a flow-through cell (Ibidi, μ-Slide I Luer, channel height 400 μm) is connected to the outlet of the reactor. A monochrome camera (IDS, UI-3080CP-M-GL) is connected to the trinocular of the stereomicroscope to record the flow behavior of the particles. The camera has a resolution of 2456 × 2054 pixels, and the pixel scale is 0.65 pixel/μm. The focus area of the microscope at 40× magnification covers half of the total flow-through area. A pulsating light source (Pyrooptic, custom-made) under the inline microscope is used to illuminate the flow-through particles and avoid blurring of the moving particles. The camera and the light pulse are controlled by using the IDS uEye software. A more detailed description of this flow-through microscopy setting can be found in this paper.[59] A flow of "push water" is added at the outlet of the reactor to push the particles to flow to the measuring cell within a very short traveling time (Table 1). The flow rate of this push water is high enough so that crystallization occurring during the traveling period can be ignored. The flow rate conditions are given in Table 1. Analyzing the recorded videos can give the induction time and nucleation rate. The video analysis is described in Section 2.4.

The above in-line microscopy allows for a partially quantitative analysis of the crystallization process. However, the particle properties such as the particle shape and size cannot be analyzed fully quantitatively because the shearing effects of the push water on the particles cannot be ignored. To further study the particle properties, three modifications are made to the setup. First, the third part of the setup is modified to add a solid collection apparatus and remove the inline microscope. As shown in Figure 1(bottom), a vacuum filtration setup (a Buchner funnel with a filter paper of 1.5 μm retention, connected to a VacuuBrand vacuum pump) is connected to the outlet of the reactor to immediately filter the outflowing slurry. It is tested beforehand whether this retention of 1.5 μm can avoid further crystallization of the particles staying on the filter paper. After filtration, the solid products are placed in the fume hood for 24 h for drying. The postanalysis including particle shape and size is discussed in Section 2.4. Second, the main body of the 20 cm tube crystallizer is extended to 60 cm (the total volume is increased from 2.5 to 7.5 mL), to have 2 times more residence time for the observation of further crystallization behavior after leaving the sonicated volume. Third, a seed slurry is introduced in the input section, and the flowing seeds are pumped to the inlet of the reactor by a Masterflex peristaltic pump (Easy-Load II pump head, flow rate range: 0.21−130 mL/min with the L/S 14 tubing). The flow rates are given in Table 3.

Table 3. Seeded and Silent Crystallization Experiments Involving Solid Collection

solution AA flow rate (mL/min)	solution HCl flow rate (mL/min)	total residence time (s)	seed slurry flow rate (mL/min)	seed loading[a] (%)	total collection time (s)
12	0.84	35.2	1.0	0.93	240
6	0.42	70.5	0.5	0.93	
6	0.42	70.5	1.0	1.87	240
3	0.21	140.9	0.5	1.87	

[a]Seed loading means the mass of seeds added compared to dissolved mass AA in the solution,[15] calculated as $\frac{\text{flow rate of seed slurry} \times \text{concentration of seed slurry}}{\text{flow rate of solution AA} \times \text{concentration of solution AA}} \times 100\%$. The concentrations of seed slurry and solution AA are 0.028 g/mL and 0.25 g/mL, respectively, mentioned in Section 2.1.

2.3. Flow Crystallization Experiments. Focusing on the question of whether applying ultrasound can replace seeding in flow reactive crystallization of AA, two aspects were investigated: inducing nucleation with ultrasound and product properties of the ultrasound-induced crystallization compared with seeds-induced products. In the study of nucleation induction, an inline microscope was used to measure the induction time and nucleation rate. First, solution AA and push water were pumped into the reactor and run for 1−2 min to get a clear background. Then, solution HCl was pumped into the reactor and ultrasound was switched on (only at sonicated conditions), in the meantime, starting the recording videos via IDS uEye software. After 5 min, all flows were stopped and the ultrasound was switched off (if present). The flow setup was cleaned completely using high flow rate of ultrapure water of 100 mL/min. Table 1 lists the conditions for the nucleation study, including two variables: sonication power and residence time. The flow ratio of solution AA and solution HCl is maintained at 100:7 which produces a mixture of pH 11.

In the study of product properties, continuous vacuum filtration was conducted to collect the solid products from both ultrasound-induced and seeds-induced crystallization. In the ultrasound-induced crystallization experiments, solution AA was first pumped into the reactor. Then, HCl and ultrasound were started in succession. The vacuum filtration was initiated immediately and ran for 5 min, with 1 min for induction and 4 min for collection. The same sonication condition was applied in two different reactors: the reactor before and after modification. The main difference between the reactors is that the modified reactor has a sonication-free volume in order to investigate further crystallization behavior after leaving the sonicated volume. Table 2 lists the conditions for the ultrasound-induced crystallization experiments. Three different flow rates are studied in each reactor.

In addition, seeds-induced crystallization experiments were performed in the modified setup for a comparative evaluation of products from ultrasound-induced crystallization. The

https://doi.org/10.1021/acs.oprd.4c00385
Org. Process Res. Dev. XXXX, XXX, XXX−XXX

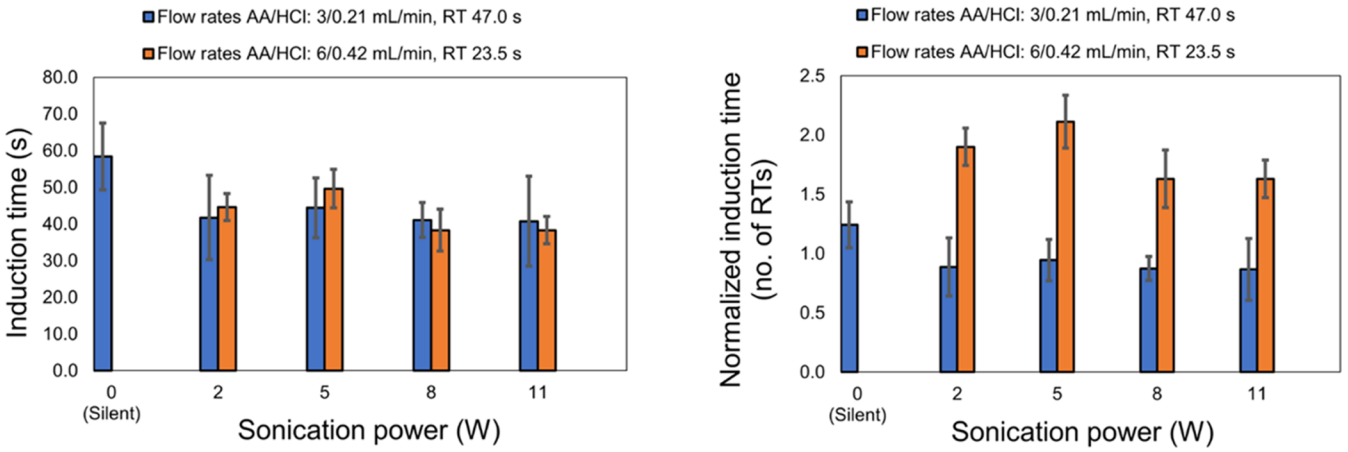

Figure 2. Induction time measurements under different sonication conditions and flow rates. The bars represent the average of triplicate experiments, and the error bars represent the standard deviation. The absence of data under the condition of "silent at flow rates AA/HCl: 6/0.42 mL/min" means no nucleation occurred.

conditions for the seeded crystallization experiments without ultrasound are listed in Table 3. The selected seed loading of below 2 wt % is suitable for small additions according to the four levels of seed loading proposed by Gong et al.[27,60] After pumping solution AA and HCl to the reactor, seed slurry was pumped in and running for a collection time of 4 min. When the flow rate of the seed slurry was set to 0.5 mL/min, part of the seeds were not flowing into the reactor but settled in the tube. Therefore, no samples were collected or analyzed in this case. Two flow conditions were repeated three times, at the flow rates of solution AA/solution HCl/seed slurry of 12/0.84/1.0 and 6/0.42/1.0 mL/min, respectively.

2.4. Analytical Methods. In this work, an inline microscope equipped with an IDS camera was used to measure the ultrasound-induced nucleation process, including induction time and nucleation rate. The videos were captured at 1 fps and extracted into images by each frame. The images were processed manually via the software ImageJ. The induction time was defined as eq 1, the three terms on the right-hand side of the equation correspond to the time of the first crystal appearing in the video, half of the residence time in the reactor, and the traveling time from the outlet of the reactor to the measuring flow-through cell, respectively. Half of the residence time was taken into account based on the assumption that nucleation takes place in the middle sections of the tube, where the ultrasound transducer is most efficient. In some experiments, the first crystal appeared, then disappeared, and appeared again in a continuous way. Only the time of continuously seen crystals appearing was considered as the induction time. This measurement was not the same as the conventional definition of the induction time, but it is used here to evaluate the reliability of ultrasound-induced nucleation because only continuously produced crystals can be accepted in real production. Additionally, the rate of increase in the number of crystals produced, considered the nucleation rate, was measured based on the growth in the total area of particles in the images over time. The particles in the image captured at each frame were selected manually via ImageJ and the total area was calculated. An example of image processing can be found in Data S3.

$$t_{\text{induction}} = t_{\text{first crystal appearing}} - t_{\text{residence}}/2 - t_{\text{traveling}} \quad (1)$$

Solid samples were collected to evaluate the ultrasound-induced crystallization process from other aspects, including crystallization yield and product properties such as particle shape and sizes. The crystallization yield was calculated following eq 2

$$\text{calculated yield (\%)} = \frac{m_{\text{contained solids}} - m_{\text{collected solids}}}{m_{\text{contained solids}}} \times 100\% \quad (2)$$

$m_{\text{collected solids}}$ is the weight of collected solids in the defined collection time and $m_{\text{contained solids}}$ is the total weight of solids contained in the solution consumed during the collection period. It is noted that the calculated yield, concerning the total mass that can be recovered with respect to the dissolved mass in the defined duration, is used to assess the effects of the experimental conditions on the crystallization process efficiency. An equilibrium concentration should be considered to calculate the maximum yield,[44] which is not the main point of this study. In addition, the particle shape was analyzed using a Scanning Electron Microscope (SEM, JEOL JSM-6010LV) after coating the samples with a gold/palladium coating using a JEOL JFC 1300 sputter coater (40 mA for 30 s). The particle sizes and size distribution were measured using a Malvern instrument (Mastersizer 3000-Hydro SV) with acetonitrile as the dispersant. The stirring speed was set at 1500 rpm. Three samples were taken for each experimental product and measured independently; therefore, the average of the three measurements was delivered as the PSD result. For assessing the reproducibility of both ultrasound-induced and seeds-induced crystallization, the standard deviation of the calculated yields and particle sizes was calculated following eq 3,

$$\text{standard deviation} = \sqrt{\frac{\sum (x - \bar{x})^2}{3}} \quad (3)$$

x and $\bar{x}$ represent the individual experimental data (calculated yield or particle size) and the average of triplicating experiments, respectively.

3. RESULTS

This work experimentally evaluated the reliability of applying ultrasound in the flow reactive crystallization of AA rather than seeding. Specifically, the possibility of ultrasound-induced

https://doi.org/10.1021/acs.oprd.4c00385
Org. Process Res. Dev. XXXX, XXX, XXX−XXX

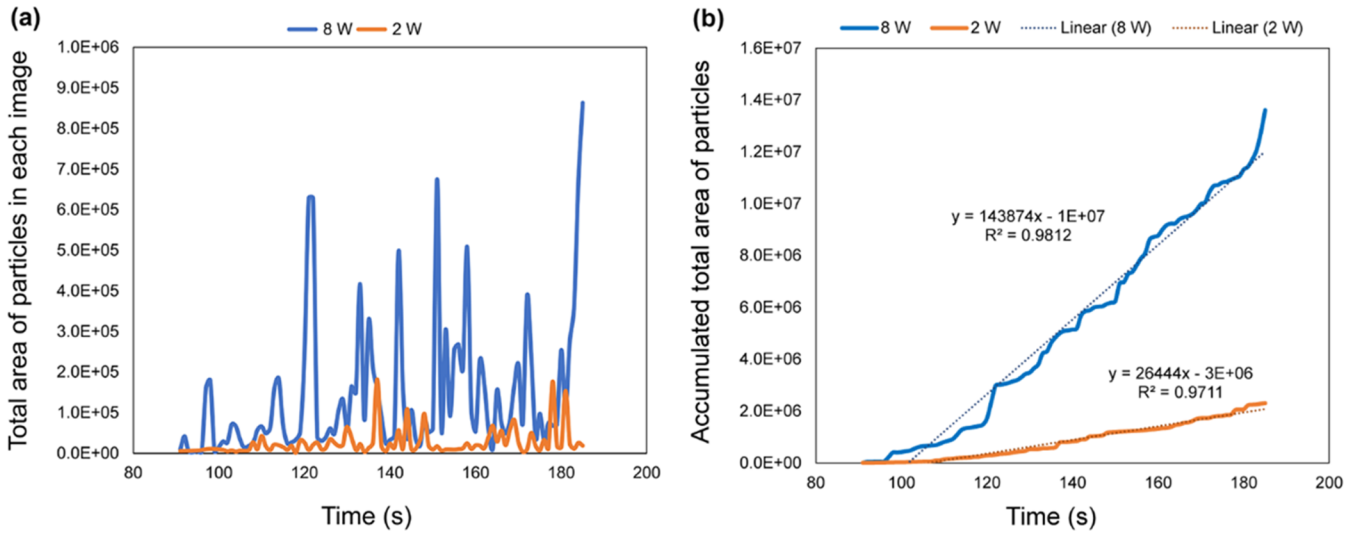

Figure 3. Nucleation rate measurement. (a) Original data of the measured total area of particles via ImageJ; (b) accumulated total area of particles at each time frame.

nucleation, the crystallization behavior of crystals leaving the induced volume, and a comparison with the conventional seeding technique were investigated. This section presents the experimental results, a comparative discussion, and the limitations of this work.

3.1. Ultrasound-Induced Nucleation. In the study of ultrasound-induced nucleation, the first step was to conduct a blank crystallization experiment without seeding or ultrasound. Solution AA and HCl were injected at the inlet and continued flowing under the silent condition. The induction time was marked when the first series of crystals was captured by the IDS camera and then calculated as eq 1. The conditions of this group of experiments, listed in Table 1, varied in flow rates (total residence time) and sonication conditions (silent, sonicated with different powers). Figure 2 shows the induction time results, including both absolute induction time measurements and the normalized induction time, which were calculated by dividing the measured induction time by the residence time. Detailed induction time data are available in Data S4.

Nucleation did happen in the silent condition when the flow of AA/HCl was slow at 3/0.21 mL/min. When the flow rates increased to 6/0.42 mL/min, there was no crystal appearing after running for 7 min. By contrast, nucleation occurred at both high and low flow rates when ultrasound was present. At a low-flow condition of 3/0.21 mL/min, the average induction time was 42.0 s under different sonication powers. The standard deviation was 1.4 s, which means there was no significant difference in the induction time among different sonication powers. The presence of ultrasound was capable of inducing nucleation even with a low power, which was within expectation and similarly reported in other application cases.[61,62] Several mechanisms behind ultrasound-assisted nucleation were proposed in the literature and most agree that introducing an ultrasound field creates cavitation bubbles in the low-frequency regime (as in this study), or acoustic streaming in the high-frequency one.[38,63,64] This mechanical effect results in the enhanced solute−solute molecular collision, which helps nucleation. It was the same for the high-flow condition; the average induction time was 42.7 s and the standard deviation was 4.8 s. Two differences in the induction time between high and low flow rates were noticed: (1) higher flow rates resulted in longer induction time, especially obviously seen in the normalized induction time, because higher flow rate induced a shorter residence time in the reactor in which case the solution may need more time to crystallize, and (2) the standard deviation of triplicating each condition shown in the error bar was smaller in the high-flow-rate case, which indicated that using ultrasound to induce nucleation was more stable and the reproducibility was better when the flow rates were high (6/0.42 mL/min). It should be noted that both flow rates here are still in the context of laminar flow.

It was observed that crystals appeared but then disappeared in silent experiments, while crystals became more and more abundant in the sonicated cases. The example videos from silent and sonicated experiments can be found in Videos S1−S3. The defined nucleation rate (the increasing rate of the number of the produced crystals) was measured based on changes in the total area of particles in each framed image over 90−180 s (this period was manually measurable in terms of particle numbers in the images—clear and concise without significant overlap). Figure 3 displays the results from sonication powers of 2 and 8 W in the case of high flow rates (6/0.42 mL/min). Figure 3a shows the original data of the measured total area of particles via ImageJ. One can see the trend that the number of particles produced increases over time, with a sonication power of 8 W generating more particles compared to 2 W. To smooth the noise of the data, the total area of particles at each time frame is accumulated, as shown in Figure 3b. Unfortunately, the particle area data could not be translated to the real nucleation rate involving the crystal mass or concentration because many overlaps were seen in the images caused by aggregation/agglomeration. Therefore, the slope of the accumulated total area of particles over time was considered as the defined nucleation rate. At this flow condition, the nucleation rate from the sonication power of 8 W was 5 times more (the ratio of slope is 5.44) compared to that of 2 W. Combining the results from induction time and nucleation rate measurements, ultrasound allows for continuous crystal production, whereas no continuous crystal formation is observed under silent conditions. The nucleation

https://doi.org/10.1021/acs.oprd.4c00385
Org. Process Res. Dev. XXXX, XXX, XXX−XXX

rate can be controlled by sonication power. Applying ultrasound in the flow crystallization of AA acts like seeding in terms of inducing crystallization.

Although higher sonication power produced more crystals, it should be noted that this may bring scaling/clogging problems. Under the condition of flow rates AA/HCl of 3/0.21 mL/min, scaling was seen at the sonication power of 5, 8, and 11 W. The problem intensified with increasing sonication power, and at 11 W, it took only 80 s for a large crystal cluster to form at the outlet due to accumulated crystals at the interface between the crystallizer and the tube. When the flow rates AA/HCl increased to 6/0.42 mL/min, scaling only occurred at a sonication power of 11 W and it took 150 s to appear since nucleation. Therefore, the problem of scaling and clogging can be reduced by increasing flow rates of AA/HCl.

3.2. Further Crystallization Behavior in Ultrasound-Induced Experiments. After the results of ultrasound-induced nucleation, the further crystallization behavior of the crystals leaving the sonication-induced volume was analyzed by the following steps. First, the solid collection was performed at the outlet of the small original reactor (2.5 mL of sonicated volume) to establish a baseline for yields and particle properties. Then, the collection experiments were conducted in the modified reactor (2.5 mL of sonicated volume and 5.0 mL of sonication-free volume). Finally, further crystallization behavior was pictured based on the comparative analysis of the achieved crystallization yields and the particle properties from the two reactors. The variables of conditions tested for these sets of experiments are flow rate and reactor type, as listed in Table 2. Except for the flow rates AA/HCl of 3/0.21 and 6/0.42 mL/min, one more condition, 12/0.84 mL/min, was conducted here. This selection was based on the experimental findings from the nucleation experiments and aimed to further prove scaling/clogging can be reduced by increasing flow rates. It was seen that the slurry flow behavior of the high-flow condition was the most fluent and had the least scaling at the same sonication condition.

Figure 4 shows the results of calculated crystallization yields from two reactors under three flow conditions. After the same collection time of 4 min, more solids were obtained in the modified reactor having a large volume, indicating that further crystallization occurred in the sonication-free volume following the ultrasound-induced nucleation in the sonicated volume. It was found that the increasing levels of additional sonication-free volume or extended residence time on crystallization yields were different among different flow conditions. At the slow-flow condition of flow rates AA/HCl 3/0.21 and 6/0.42 mL/min, in the modified reactor with longer residence time, the crystallization yield increased from 5.17 to 20.73% and from 4.20 to 8.14%, respectively. While at the high flow rates of AA/HCl 12/0.84 mL/min, there was only a slight increase from 6.26% to 7.63% compared to the collection results in the original reactor of 2.5 mL. The higher flow rates led to less increase in crystallization yields due to the shorter residence time and shorter sonication time. Besides, one can see that the standard deviation at the high flow rates of 12/0.84 mL/min was smaller compared to that of the other two flow conditions, implying higher reliability and reproducibility under high-flow conditions. Therefore, adopting high-flow conditions is better when taking the reliability and clogging problem into account, and increasing the sonication power can help to improve the crystallization yields if desired.

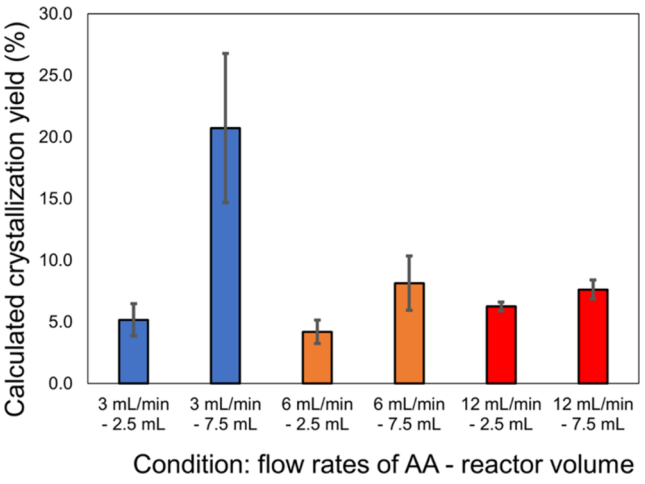

Figure 4. Calculated crystallization yield results from two reactors under different flow conditions: flow rates AA/HCl of 3/0.21 mL/min, 6/0.42 mL/min, and 12/0.84 mL/min (only the flow rate of AA is shown on the axis label). Two reactors are the 2.5 mL sonicated reactor and the modified reactor with 2.5 mL sonicated volume and 5 mL sonication-free volume, respectively. Applied ultrasound condition: frequency 42.8 kHz, amplitude 180 mVpp, sonication power 8 W. The bars represent the average of triplicate experiments, and the error bars represent the standard deviation.

The particle sizes and size distribution were analyzed to understand the ultrasound-induced crystallization process. The modified reactor had an additional 5 mL sonication-free volume which provided 2 times more residence time. Figure 5 shows the particle size distributions of samples from two reactors under different flow conditions. At a flow condition AA/HCl of 3/0.21 mL/min, the particle size shifted from a bimodal distribution (2.5 mL reactor) to a unimodal distribution (7.5 mL reactor) with a peak position of 58.9 μm and a narrow span of 2.4. At a flow condition AA/HCl of 6/0.42 mL/min, the particles from both reactors had a unimodal distribution while the peak position moved from 186 to 127 μm in the large reactor. At the flow rates AA/HCl of 12/0.84 mL/min, two reactors gave similar particle size distribution results with two close peak positions at 111 μm (2.5 mL reactor) and 144 μm (7.5 mL reactor). Combined with the average particle sizes present in Table 4, it was found that the particles collected in the large reactor contained more small particles with a narrow span, which indicated that secondary nucleation predominated the further crystallization process after ultrasound-induced nucleation. This effect was due to crystallization yields exceeding 5% in the small reactor, which was equivalent to a seed loading of over 5% in the large reactor, thereby favoring secondary nucleation. In addition, one can see from the case of fast flow condition (flow rates of AA/HCl 12/0.84 mL/min), that the particles obtained from both small and large reactors appeared to have similar size properties, meaning that stable crystal production throughout the crystallization process was achieved under this condition. Therefore, integrating the observation of the scaling/clogging problem, the crystallization yield measurement, and the particle size and size distribution analysis, a higher flow condition is preferable when using ultrasound as a seeding technique.

3.3. Comparative Study with Seeds-Induced Crystallization. Based on the analysis of ultrasound-induced crystallization, applying ultrasound is capable of continuously

https://doi.org/10.1021/acs.oprd.4c00385
Org. Process Res. Dev. XXXX, XXX, XXX−XXX

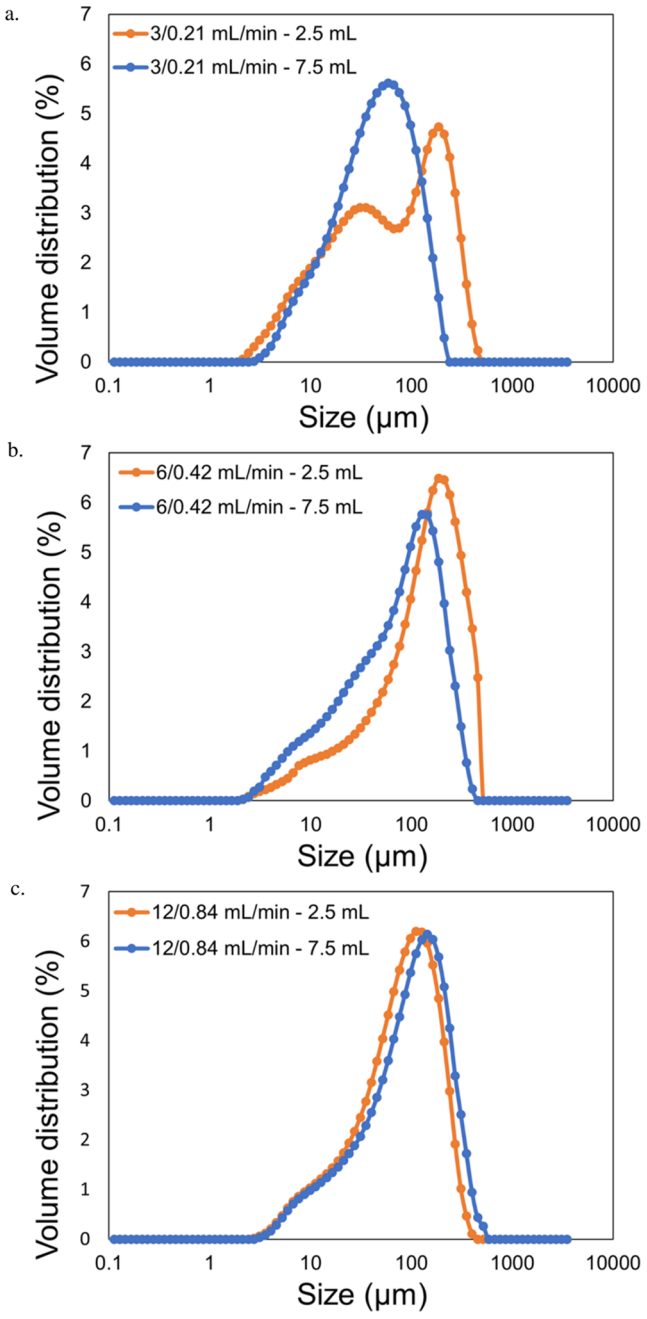

Figure 5. Particle size distribution results from two reactors under different flow conditions: (a) flow rates of solution AA/HCl: 3/0.21 mL/min, (b) flow rates of solution AA/HCl: 6/0.42 mL/min, and (c) flow rates of solution AA/HCl: 12/0.84 mL/min. Two reactors are the 2.5 mL sonicated reactor and the modified reactor with 2.5 mL sonicated volume and 5 mL sonication-free volume, respectively. Applied ultrasound condition: frequency 42.8 kHz, amplitude 180 mVpp, sonication power 8 W.

producing crystals with a suitable size distribution. Under specific flow conditions, applying appropriate sonication conditions can reduce the scaling/clogging problem and balance the crystallization rates. Therefore, it is reasonable to conclude that using ultrasound can be as effective as using seeds in the flow reactive crystallization of AA. The last part of this work was to conduct sets of seeds-induced crystallization experiments for comparative study with using ultrasound. The seeded experiment conditions are described in Table 32.3. The

Table 4. Average Sizes of Particles from the Two Reactors under Different Flow Conditions

experimental condition: flow rates of AA/HCl − reactor type[a]	Dx_10 (μm)	Dx_50 (μm)	Dx_90 (μm)	span
3/0.21 mL/min − 2.5 mL	9.55	64.9	259.5	3.9
3/0.21 mL/min − 7.5 mL	12.1	48	128	2.4
6/0.42 mL/min − 2.5 mL	24.8	157.0	339.3	2.0
6/0.42 mL/min − 7.5 mL	12.2	85.1	222.0	2.5
12/0.84 mL/min − 2.5 mL	17.8	88.5	216.3	2.2
12/0.84 mL/min − 7.5 mL	22.1	111.5	262.3	2.2

[a]Reactor type includes a 2.5 mL sonicated reactor and a modified reactor with 2.5 mL sonicated volume and 5 mL sonication-free volume. Applied ultrasound condition: frequency 42.8 kHz, amplitude 180 mVpp, sonication power 8 W.

case of low flow rates of AA/HCl of 3/0.21 mL/min was not desired considering the results from the previous sections and therefore not included in seeded experiments. The experiments were conducted at two flow conditions: flow rates AA/HCl/seeds of 6/0.42/1.0 mL/min and 12/0.84/1.0 mL/min, and the calculated crystallization yields after the same collection duration of 4 min and the corresponding particle properties were analyzed. As shown in Figure 6, in the seeded

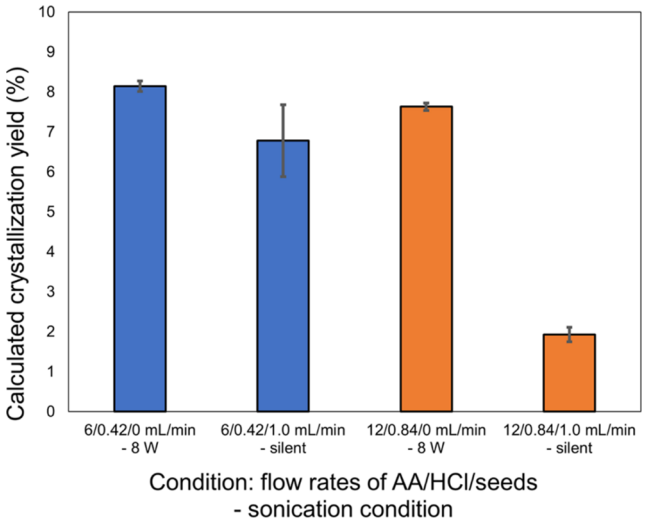

Figure 6. Calculated crystallization yield results from ultrasound-induced and seed-induced crystallization experiments. The sonicated experiment results are copied from the previous sections and put together with the seeded experiments for comparison. The bars represent the average of triplicate experiments, and the error bars represent the standard deviation.

experiments, the crystallization yield of low flow rates 6/0.42 mL/min was higher compared to that of high flow rates 12/0.84, mainly because the seed slurry of 1.0 mL/min gave a higher seed loading of 1.87% for the case of slow flow in comparison with 0.93% for the case of fast flow. At both flow conditions, ultrasound-induced crystallization achieved higher yields but also had a smaller standard deviation compared with seeds-induced crystallization. Therefore, within the scope of the experimental conditions studied, using ultrasound is better than seeding from the perspective of crystallization yields.

Particle sizes and size distribution results are listed in Figure 7 and Table 5. It was found that both flow rates of solution and seed loading influenced the crystallization process. The seeded experiments at the slow-flow condition (flow rates AA/HCl/

https://doi.org/10.1021/acs.oprd.4c00385
Org. Process Res. Dev. XXXX, XXX, XXX−XXX

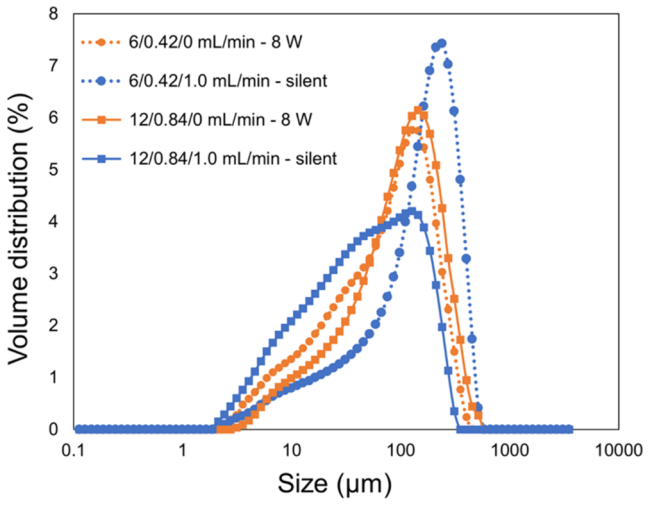

Figure 7. PSD result of ultrasound-induced and seed-induced crystallization experiments. The sonicated experiment results are copied from the previous sections.

Table 5. Average Sizes of Particles from Ultrasound-Induced and Seeds-Induced Crystallization

condition: flow rates of AA/HCl/seeds (mL/min)	Dx_10 (μm)	Dx_50 (μm)	Dx_90 (μm)	span
6/0.42/0 − 8 W	12.2	85.1	222.0	2.5
6/0.42/1.0 − silent	21.1	168.5	353.0	2.0
12/0.84/0 − 8 W	22.1	111.5	262.3	2.2
12/0.84/1.0 − silent	8.33	51.1	184	3.4

seeds: 6/0.42/1.0 mL/min, with a higher seed loading of 1.87%) produced more large particles with a narrow unimodal distribution of 2.0. It could be agglomeration caused by the high seed loading and relatively long residence time. In the same flow condition but with ultrasound, there were not many large particles probably because of deagglomeration effects by sonication. The average sizes of particles obtained from the fast flow condition (flow rates AA/HCl/seeds: 12/0.84/1.0 mL/min, with a lower seed loading of 0.93%) were rather small and the size distribution was too broad without a well-defined peak position. This could be the result of low seed loading and short residence time. By contrast, the particles from sonicated experiments at both flow conditions had a unimodal and narrow size distribution. Combining the results of crystallization yields, one can conclude using ultrasound is more reliable and easier to control the particle properties compared to seeding crystals in flow reactive crystallization of AA. A detailed discussion of ultrasound-induced crystallization versus seed-induced crystallization is provided in Section 4.1.

3.4. SEM Analysis of Particle Shape. In this study, the particle shape was analyzed by using SEM. Figure 8 displays the SEM images from both sonicated and seeded experiments. The particle shape appeared the same—a porous particle. Sonication did not change the particle shape or form. On the other hand, the presence of fine particles on the surface of the large particle could be a second indication of secondary nucleation, besides the particle size distribution analysis in Section 3.2. According to SEM analysis, using ultrasound or seeding works the same from the aspect of the particle shape.

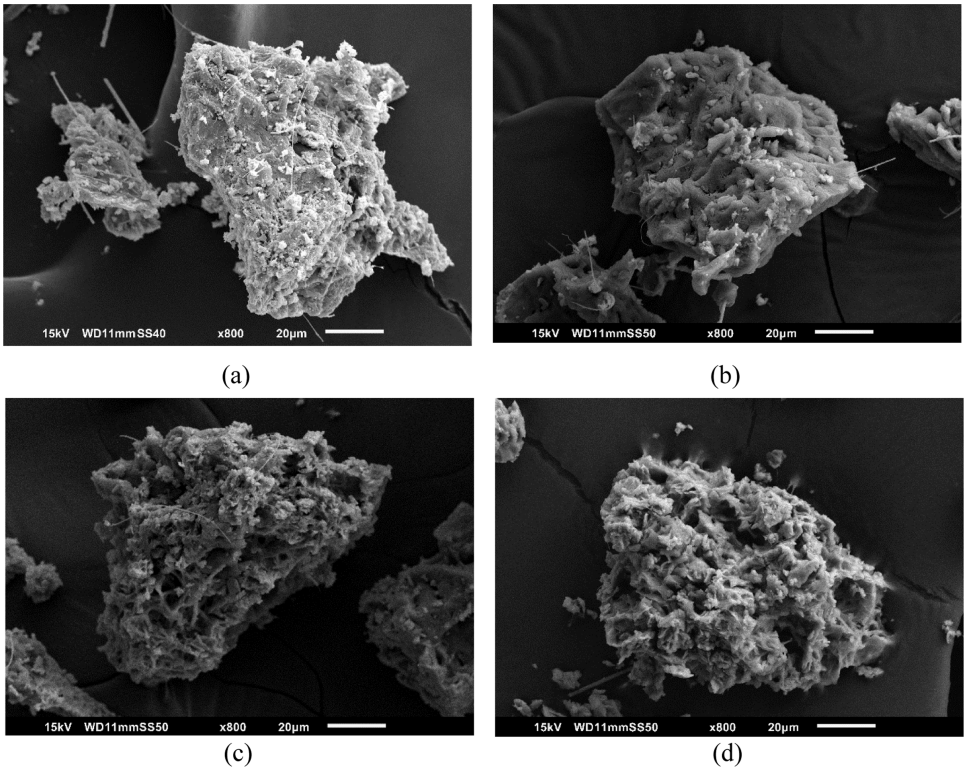

Figure 8. SEM images of particles from ultrasound-induced crystallization and seeds-induced crystallization. Flow rates of AA/HCl/seeds (mL/min)—sonication condition: (a) 6/0.42/0 − 8 W, (b) 6/0.42/1.0 − silent, (c) 12/0.84/0 − 8 W, and (d) 12/0.84/1.0 − silent.

https://doi.org/10.1021/acs.oprd.4c00385
Org. Process Res. Dev. XXXX, XXX, XXX−XXX

(a) Flow rate of seed slurry 1.0 mL/min

(b) Flow rate of seed slurry 0.5 mL/min

Figure 9. Images showing flowing behaviors of seed slurry under different flow conditions. The solid content is 2.8% w/v, as explained in Section 2.1.

4. DISCUSSION

4.1. Comparative Discussion on Using Ultrasound Rather Than Seeding. The experiments designed in this work are aimed at answering the question of whether ultrasound can be used in the flow reactive crystallization of AA as an alternative seeding technique. This question is addressed from three perspectives: whether ultrasound can be used for inducing nucleation; if so, how the crystals develop after nucleation; and finally, how is this approach compared to the conventional seeding technique? One can see from the results in Sections 3.1−3.4, that the introduction of ultrasound enables stable nucleation−continuously producing crystals. The nucleation rate under this approach can be controlled simply by adjusting the sonication power. The slurry containing the formed nuclei continues to crystallize after leaving the ultrasound-induced volume, which is proven by the two sets of experiments conducted in different reactors: one set in the small tubular reactor with only the sonicated volume and the other set in the extended reactor with an additional sonication-free volume and total triple length. The particles obtained from the extended reactor exhibit a smaller average size compared with the particles from the small reactor. One possible explanation for this is that secondary nucleation predominates during the further crystallization process rather than crystal growth. Compared to the seeds-induced crystallization experiments, applying ultrasound is able to achieve higher yields without changing the porous particle shape and also to produce narrow-span products with desired sizes. Last but not least, the ultrasound-induced experiments are quite reproducible, as indicated by the standard deviation analysis, which implies the reliability of using ultrasound in this flow crystallization system as a replacement for the conventional seeding technique.

Although the experimental findings demonstrate the effectiveness of using ultrasound as seeds, it is worth comparing the operational differences between using ultrasound and seeding. In this work, seed-induced crystallization experiments are difficult to control mainly due to the operation of the pumping seed slurry. The solids are highly likely to sediment, which makes it difficult to get a stable seeding flow with the determined solid content. Figure 9 gives examples of different flowing behaviors of seed slurry. With a seed flow rate of 1.0 mL/min, the flow is still normal. However, with the seed flow rate of 0.5 mL/min, Figure 9b clearly shows the sedimentation of seeds in the tube of lower position, resulting in insufficient seeds entering the inlet of the reactor. Sultana et al.[26] also reported this difficulty in pumping seeds of high-density particles such as α-glycine. By contrast, the operation of using ultrasound to induce crystallization is quite efficient and robust simply by setting the frequency and amplitude of the ultrasound. Still, the parameters should be tested in advance to achieve a moderate crystallization rate for the specific flow conditions with the consideration of potential scaling/clogging problems.

4.2. General Discussion on the Feasibility of Applying Ultrasound as a Seeding Technique. Generally, continuous in situ seed generation, eliminating the need for preparation of seed materials and subsequent resuspension and transport, is preferable over conventional seeding crystals into the system for a long-time continuous operation and is more sustainable and economical. Using sonication would be advantageous due to its ease of controlling the generation rate and quality, thus generating a reliable and robust continuous process. Despite these presented benefits of using ultrasound, it is noted that several critical factors should be assessed before moving to an industrial scale, such as the design of suitable ultrasound equipment, the potential foreign particles from surface erosion, and the continuous crystallizer for scaling up. Direct contact of ultrasound with the process solution has a high risk of particle shedding due to surface erosion as reported in the literature.[65] An indirect and contact-free ultrasonic treatment, seen in the works of Jiang[53] and Yang,[47] can be preferred, especially in the manufacturing of pharmaceuticals. However, the foreign particles might be generated from the irradiated reactor surface erosion,[39] which indicates the significance of evaluating the risk of shedding of the reactor wall surfaces. Furthermore, one has to combine the in situ ultrasound-induced seed generator with a suitable industrial continuous crystallizer. For example, the easily scalable COBC reported in the literature,[66−68] could be considered for scaling up to pilot-scale and even industrial-sized production.

4.3. Limitations of This Study. Overall, it is concluded in this study that using ultrasound has benefits over seeding in flow crystallization of AA and other compounds with a similar nature. However, based on the observations in the experiments, it is important to discuss certain limitations of this study and several improvements that can be made in future studies.

4.3.1. Reactor Design. In this work, the two tubular reactors have the same shape with different lengths; the longer one has an extended sonication-free volume to study further crystallization behavior. There are two limitations to this design: (a) the ultrasound transducer is directly attached to the bottom of the sonicated volume, while ultrasonic vibration can continue to propagate forward to the sonication-free volume, which is not explicitly accounted for in the analysis; and (b) both reactors have only one inlet and one outlet in which case the flow ratio cannot be adjusted during the flow crystallization

https://doi.org/10.1021/acs.oprd.4c00385
Org. Process Res. Dev. XXXX, XXX, XXX−XXX

process. The selected flow ratio of this study led to a slurry of pH 11. This pH is suitable as the seeding pH or pH of inducing nucleation, but it is not the final pH for neutralizing the solution AA completely. This consideration does not conflict with the experimental findings and conclusions of this work. Still, it is recommended to build a setup that connects an ultrasound-induced reactor for nucleation to a separate reactor for complete neutralization and further crystallization. For instance, it would be advantageous to integrate an ultrasound-induced nucleator with a continuous oscillatory baffled crystallizer that could design several inlets for reactant injection and outlets for sample analysis.

4.3.2. Flow-Through Microscopy. An in-line microscope was used to measure the induction time and nucleation rate in this work. Although this basic goal is achieved, there are some other functions of the microscope reported in the literature, such as particle size and agglomeration degree analysis.[55,59] The limitation in this reactive crystallization system lies within the dilution solution; both water and saturated solution failed to work as a proper dilution solution, which cannot dissolve the crystals nor make crystallization happen. In the end, high-flow push water was introduced at the outlet of the reactor, pushing the crystals to flow to the measuring channel within a short traveling time yet making the particle size measurements via flow-through microscopy not applicable. For the future study of this compound and other similar studies on reactive crystallization systems, a suitable buffer solution with the same pH and without any interactions with the studied system could be a potential dilution solution, which might help make full use of flow-through microscopy.

4.3.3. Limitation on General Application. This study proves that using ultrasound can be an alternative seeding technique. However, this particular reactive crystallization system does not involve polymorphs. Other compounds, especially pharmaceuticals, are likely to have more than one form, in which case adding seeds of the specific form might be necessary for polymorph control in flow crystallization. Nonetheless, with the help of ultrasound, using seeds can be more effective. For example, Hussain et al.[44] reported that seeding is only effective under sonicated conditions for the production of the most stable form of *ortho*-aminobenzoic acid (*o*-ABA). Besides, the solubility of compound AA is mainly pH-dependent, and the temperature does not affect the solubility within the temperature around 25 °C, which makes the slight temperature increase caused by sonication negligible. If ultrasound is applied in a flow-cooling crystallization system, corresponding measures should be taken to strictly control the temperature in the sonicated volume, which might be energy-consuming.

5. CONCLUSIONS

In this work, reactive crystallization experiments of AA in a flow reactor were conducted under these conditions: silent without seeds, sonicated without seeds, and silent with seeds. It was found that in the case of silent crystallization without seeds there were no continuously produced crystals even though nucleation happened in certain conditions. Under sonication conditions without seeds, ultrasound successfully induced stable nucleation under different flow conditions. The nucleation rate can be manipulated by adjusting the sonication power. The nuclei allowed the slurry to further crystallize in the art of a dominating secondary nucleation, and the final products achieved a suitable size distribution and well-maintained particle shape. The function of ultrasound behaved like seeds from the perspective of initializing crystallization and producing the desired products. Compared with seeded experiments, sonicated experiments had the main advantages of easy operation and reliable reproducibility. Therefore, it can be concluded that ultrasound can be used as a replacement for conventional seeding techniques in the flow crystallization of the compound Aromatic Amine and other similar crystallization systems. A further strength of the sonication-enabled in situ seed generation strategy is its high efficiency and robustness regardless of flow conditions, as a result contributing to the development of advanced crystallization technology. The concept of the reactor design integrating ultrasound with flow to make an easy-control crystallization process and scale-up needs further study and development, which is among future research plans.

■ ASSOCIATED CONTENT

Supporting Information

The Supporting Information is available free of charge at https://pubs.acs.org/doi/10.1021/acs.oprd.4c00385.

Information about sodium acetate (S1); example of temperature profile (S2); image processing example (S3); induction time data (S4); and link to the supplementary videos (S5). (PDF)

■ AUTHOR INFORMATION

Corresponding Author

Tom Van Gerven − *Department of Chemical Engineering, Process Engineering for Sustainable Systems, KU Leuven, 3001 Heverlee, Belgium;* orcid.org/0000-0003-2051-5696; Email: tom.vangerven@kuleuven.be

Authors

Biyu Zhang − *Department of Chemical Engineering, Process Engineering for Sustainable Systems, KU Leuven, 3001 Heverlee, Belgium;* orcid.org/0000-0002-3963-3900

Georgios D. Stefanidis − *Department of Process Analysis and Plant Design, School of Chemical Engineering, National Technical University of Athens, 15780 Athens, Greece*

Complete contact information is available at: https://pubs.acs.org/10.1021/acs.oprd.4c00385

Author Contributions

B.Z.: conceptualization, methodology, investigation, data curation, software, validation, visualization, writing— original draft, review and editing. G.D.S.: methodology, writing—review and editing, supervision, funding acquisition. T.V.G.: conceptualization, methodology, project administration, resources, writing—review and editing, supervision, funding acquisition.

Funding

The research leading to these results has received funding from the European Union's Horizon Research and Innovation Programmes under Grant Agreement No. 101058279 (SIMPLI-DEMO). This publication reflects only the authors' view, exempting the Community from any liability. Project Web site: https://simpli-demo.eu/.

Notes

The authors declare no competing financial interest.

■ ACKNOWLEDGMENTS

We are thankful to GE HealthCare (Lindesnes, Norway) for their generous donation of the compound. We are also thankful to Prof. Leen Braeken at Chemical Process Technology TC, Diepenbeek Campus of KU Leuven, for giving access to their microscope. We are also thankful to Dr. Arne Vancleef for the helpful guidance on the flow-through microscopy.

■ REFERENCES

(1) Myerson, A. S.; Erdemir, D.; Lee, A. Y. *Handbook of Industrial Crystallization*; Myerson, A. S.; Erdemir, D.; Lee, A. Y., Eds.; Cambridge University Press, 2019.
(2) Lewis, A.; Seckler, M.; Kramer, H.; van Rosmalen, G. *Industrial Crystallization*; Cambridge University Press, 2015.
(3) Shores, B. T.; Sieg, P. E.; Nicosia, A. T.; Hu, C.; Born, S. C.; Shvedova, K.; Sayin, R.; Testa, C. J.; Wu, W.; Takizawa, B.; Ramanujam, S.; Mascia, S. Design of a Continuous Solvent Recovery System for End-to-End Integrated Continuous Manufacturing of Pharmaceuticals. *Org. Process Res. Dev.* **2020**, *24* (10), 1996−2003.
(4) Hu, C.; Testa, C. J.; Born, S. C.; Wu, W.; Shvedova, K.; Sayin, R.; Halkude, B. S.; Casati, F.; Ramnath, A.; Hermant, P.; Takizawa, B.; O'Connor, T. F.; Yang, X.; Ramanujam, S.; Mascia, S. E-Factor Analysis of a Pilot Plant for End-to-End Integrated Continuous Manufacturing (ICM) of Pharmaceuticals. *Green Chem.* **2020**, *22* (13), 4350−4356.
(5) Balogh, A.; Domokos, A.; Farkas, B.; Farkas, A.; Rapi, Z.; Kiss, D.; Nyiri, Z.; Eke, Z.; Szarka, G.; Örkényi, R.; Mátravölgyi, B.; Faigl, F.; Marosi, G.; Nagy, Z. K. Continuous End-to-End Production of Solid Drug Dosage Forms: Coupling Flow Synthesis and Formulation by Electrospinning. *Chem. Eng. J.* **2018**, *350*, 290−299.
(6) Adamo, A.; Beingessner, R. L.; Behnam, M.; Chen, J.; Jamison, T. F.; Jensen, K. F.; Monbaliu, J. C. M.; Myerson, A. S.; Revalor, E. M.; Snead, D. R.; Stelzer, T.; Weeranoppanant, N.; Wong, S. Y.; Zhang, P. On-Demand Continuous-Flow Production of Pharmaceuticals in a Compact, Reconfigurable System. *Science* **2016**, *352* (6281), 61−67.
(7) Eren, A.; Civati, F.; Ma, W.; Gamekkanda, J. C.; Myerson, A. S. Continuous Crystallization and Its Potential Use in Drug Substance Manufacture: A Review. *J. Cryst. Growth* **2023**, *601*, No. 126958.
(8) Pu, S.; Hadinoto, K. Continuous Crystallization as a Downstream Processing Step of Pharmaceutical Proteins: A Review. *Chem. Eng. Res. Des.* **2020**, *160*, 89−104.
(9) Orehek, J.; Teslić, D.; Likozar, B. Continuous Crystallization Processes in Pharmaceutical Manufacturing: A Review. *Org. Process Res. Dev.* **2021**, *25* (1), 16−42.
(10) Zhao, B.; Zang, H.; Zhong, L.; Ma, X.; Wang, H.; Zhang, H.; Li, L. Review of the Application of PAT in the Pharmaceutical Continuous Crystallization Process. *Curr. Top. Med. Chem.* **2023**, *23* (18), 1699−1714.
(11) Wood, B.; Girard, K. P.; Polster, C. S.; Croker, D. M. Progress to Date in the Design and Operation of Continuous Crystallization Processes for Pharmaceutical Applications. *Org. Process Res. Dev.* **2019**, *23* (2), 122−144.
(12) Jiang, M.; Braatz, R. D. Designs of Continuous-Flow Pharmaceutical Crystallizers: Developments and Practice. *CrystEngComm* **2019**, *21* (23), 3534−3551.
(13) Darmali, C.; Mansouri, S.; Yazdanpanah, N.; Woo, M. W. Mechanisms and Control of Impurities in Continuous Crystallization: A Review. *Ind. Eng. Chem. Res.* **2019**, *58* (4), 1463−1479.
(14) Acevedo, D.; Yang, X.; Liu, Y. C.; O'Connor, T. F.; Koswara, A.; Nagy, Z. K.; Madurawe, R.; Cruz, C. N. Encrustation in Continuous Pharmaceutical Crystallization Processes—A Review. *Org. Process Res. Dev.* **2019**, *23* (6), 1134−1142.
(15) Liu, F.; Bagi, S. D.; Su, Q.; Chakrabarti, R.; Barral, R.; Gamekkanda, J. C.; Hu, C.; Mascia, S. Targeting Particle Size Specification in Pharmaceutical Crystallization: A Review on Recent Process Design and Development Strategies and Particle Size Measurements. *Org. Process Res. Dev.* **2022**, *26* (12), 3190−3203.
(16) Gao, Z.; Wu, Y.; Gong, J.; Wang, J.; Rohani, S. Continuous Crystallization of α-Form L-Glutamic Acid in an MSMPR-Tubular Crystallizer System. *J. Cryst. Growth* **2019**, *507*, 344−351.
(17) Briggs, N. E. B.; Schacht, U.; Raval, V.; McGlone, T.; Sefcik, J.; Florence, A. J. Seeded Crystallization of β-L-Glutamic Acid in a Continuous Oscillatory Baffled Crystallizer. *Org. Process Res. Dev.* **2015**, *19* (12), 1903−1911.
(18) Giri, G.; Yang, L.; Mo, Y.; Jensen, K. F. Adding Crystals To Minimize Clogging in Continuous Flow Synthesis. *Cryst. Growth Des.* **2019**, *19* (1), 98−105.
(19) Termühlen, M.; Etmanski, M. M.; Kryschewski, I.; Kufner, A. C.; Schembecker, G.; Wohlgemuth, K. Continuous Slug Flow Crystallization: Impact of Design and Operating Parameters on Product Quality. *Chem. Eng. Res. Des.* **2021**, *170*, 290−303.
(20) Hohmann, L.; Greinert, T.; Mierka, O.; Turek, S.; Schembecker, G.; Bayraktar, E.; Wohlgemuth, K.; Kockmann, N. Analysis of Crystal Size Dispersion Effects in a Continuous Coiled Tubular Crystallizer: Experiments and Modeling. *Cryst. Growth Des.* **2018**, *18* (3), 1459−1473.
(21) Binev, D.; Seidel-Morgenstern, A.; Lorenz, H. Continuous Separation of Isomers in Fluidized Bed Crystallizers. *Cryst. Growth Des.* **2016**, *16* (3), 1409−1419.
(22) Binev, D.; Seidel-Morgenstern, A.; Lorenz, H. Study of Crystal Size Distributions in a Fluidized Bed Crystallizer. *Chem. Eng. Sci.* **2015**, *133*, 116−124.
(23) Du, X.; Xie, C.; Liu, B.; Yuan, P.; Sun, H. Continuous Crystallization Process of Cefminox Sodium in MSMPR Crystallizer. *Cryst. Res. Technol.* **2023**, *58* (4), No. 2200256.
(24) Pu, S.; Hadinoto, K. Comparative Evaluations of Bulk Seeded Protein Crystallization in Batch versus Continuous Slug Flow Crystallizers. *Chem. Eng. Res. Des.* **2021**, *171*, 139−149.
(25) Steenweg, C.; Kufner, A. C.; Habicht, J.; Wohlgemuth, K. Towards Continuous Primary Manufacturing Processes—Particle Design through Combined Crystallization and Particle Isolation. *Processes* **2021**, *9* (12), 2187.
(26) Sultana, M.; Jensen, K. F. Microfluidic Continuous Seeded Crystallization: Extraction of Growth Kinetics and Impact of Impurity on Morphology. *Cryst. Growth Des.* **2012**, *12* (12), 6260−6266.
(27) He, Y.; Gao, Z.; Zhang, T.; Sun, J.; Ma, Y.; Tian, N.; Gong, J. Seeding Techniques and Optimization of Solution Crystallization Processes. *Org. Process Res. Dev.* **2020**, *24* (10), 1839−1849.
(28) Eder, R. J. P.; Schmitt, E. K.; Grill, J.; Radl, S.; Gruber-Woelfler, H.; Khinast, J. G. Seed Loading Effects on the Mean Crystal Size of Acetylsalicylic Acid in a Continuous-flow Crystallization Device. *Cryst. Res. Technol.* **2011**, *46* (3), 227−237.
(29) Yazdanpanah, N.; Nagy, Z. K. *The Handbook of Continuous Crystallization*; Yazdanpanah, N.; Nagy, Z. K., Eds.; The Royal Society of Chemistry, 2020.
(30) Beckmann, W. *Crystallization: Basic Concepts and Industrial Applications*; Beckmann, W., Ed.; Wiley, 2013.
(31) Jiang, M.; Wong, M. H.; Zhu, Z.; Zhang, J.; Zhou, L.; Wang, K.; Ford Versypt, A. N.; Si, T.; Hasenberg, L. M.; Li, Y.-E.; Braatz, R. D. Towards Achieving a Flattop Crystal Size Distribution by Continuous Seeding and Controlled Growth. *Chem. Eng. Sci.* **2012**, *77*, 2−9.
(32) Johnson, B. K.; Prud'homme, R. K. Chemical Processing and Micromixing in Confined Impinging Jets. *AIChE J.* **2003**, *49* (9), 2264−2282.
(33) Mahajan, A. J.; Kirwan, D. J. Nucleation and Growth Kinetics of Biochemicals Measured at High Supersaturations. *J. Cryst. Growth* **1994**, *144* (3−4), 281−290.
(34) Wu, W.-L.; Oliva, J. A.; Kshirsagar, S.; Burcham, C. L.; Nagy, Z. K. Continuous In Situ Seed Generation through the Integration of a Mixed Suspension Mixed Product Removal and an Oscillatory Baffled Crystallizer for the Control of Crystal Size Distribution and Polymorphic Form. *Cryst. Growth Des.* **2021**, *21* (12), 6684−6696.

https://doi.org/10.1021/acs.oprd.4c00385
Org. Process Res. Dev. XXXX, XXX, XXX−XXX

(35) Qamar, S.; Peter Elsner, M.; Hussain, I.; Seidel-Morgenstern, A. Seeding Strategies and Residence Time Characteristics of Continuous Preferential Crystallization. *Chem. Eng. Sci.* **2012**, *71*, 5−17.
(36) Adamou, P.; Harkou, E.; Villa, A.; Constantinou, A.; Dimitratos, N. Ultrasonic Reactor Set-Ups and Applications: A Review. *Ultrason. Sonochem.* **2024**, *107*, No. 106925.
(37) Banakar, V. V.; Sabnis, S. S.; Gogate, P. R.; Raha, A.; Saurabh. Ultrasound Assisted Continuous Processing in Microreactors with Focus on Crystallization and Chemical Synthesis: A Critical Review. *Chem. Eng. Res. Des.* **2022**, *182*, 273−289.
(38) Jordens, J.; Gielen, B.; Xiouras, C.; Hussain, M. N.; Stefanidis, G. D.; Thomassen, L. C. J.; Braeken, L.; Van Gerven, T. Sonocrystallisation: Observations, Theories and Guidelines. *Chem. Eng. Process. − Process Intensif.* **2019**, *139*, 130−154.
(39) Sander, J. R. G.; Zeiger, B. W.; Suslick, K. S. Sonocrystallization and Sonofragmentation. *Ultrason. Sonochem.* **2014**, *21* (6), 1908−1915.
(40) Ruecroft, G.; Hipkiss, D.; Ly, T.; Maxted, N.; Cains, P. W. Sonocrystallization: The Use of Ultrasound for Improved Industrial Crystallization. *Org. Process Res. Dev.* **2005**, *9* (6), 923−932.
(41) Zhao, S.; Zhao, Q.; Yao, C.; Chen, G. Investigation of Anti-Clogging Mechanism of Ultrasound-Driven Oscillating Slugs/Bubbles and Its Application on Continuous Crystallization Process. *Chem. Eng. Sci.* **2024**, *290*, No. 119898.
(42) Liao, H.; Huang, W.; Zhou, L.; Fang, L.; Gao, Z.; Yin, Q. Ultrasound-Assisted Continuous Crystallization of Metastable Polymorphic Pharmaceutical in a Slug-Flow Tubular Crystallizer. *Ultrason. Sonochem.* **2023**, *100*, No. 106627.
(43) Fang, L.; Gao, Z.; Gao, Z.; Huang, W.; Wan, X.; Rohani, S.; Gong, J. Controlled Crystallization of Metastable Polymorphic Pharmaceutical: Comparative Study of Batchwise and Continuous Tubular Crystallizers. *Chem. Eng. Sci.* **2023**, *266*, No. 118277.
(44) Hussain, M. N.; Jordens, J.; Kuhn, S.; Braeken, L.; Van Gerven, T. Ultrasound as a Tool for Polymorph Control and High Yield in Flow Crystallization. *Chem. Eng. J.* **2021**, *408*, No. 127272.
(45) Hussain, M. N.; Baeten, S.; Jordens, J.; Braeken, L.; Van Gerven, T. Process Intensified Anti-Solvent Crystallization of o-Aminobenzoic Acid via Sonication and Flow. *Chem. Eng. Process. − Process Intensif.* **2020**, *149*, No. 107823.
(46) Zhao, Q.; Yang, L.; Yao, C.; Chen, G. Ultrasonic Enhanced Continuous Crystallization: Induction Time and Process Control. *Ind. Eng. Chem. Res.* **2023**, *62* (47), 20083−20095.
(47) Yang, Y.; Ahmed, B.; Mitchell, C.; Quon, J. L.; Siddique, H.; Houson, I.; Florence, A. J.; Papageorgiou, C. D. Investigation of Wet Milling and Indirect Ultrasound as Means for Controlling Nucleation in the Continuous Crystallization of an Active Pharmaceutical Ingredient. *Org. Process Res. Dev.* **2021**, *25* (9), 2119−2132.
(48) Jordens, J.; Canini, E.; Gielen, B.; Van Gerven, T.; Braeken, L. Ultrasound Assisted Particle Size Control by Continuous Seed Generation and Batch Growth. *Crystals* **2017**, *7* (7), 195.
(49) Furuta, M.; Mukai, K.; Cork, D.; Mae, K. Continuous Crystallization Using a Sonicated Tubular System for Controlling Particle Size in an API Manufacturing Process. *Chem. Eng. Process. − Process Intensif.* **2016**, *102*, 210−218.
(50) Eder, R. J. P.; Schrank, S.; Besenhard, M. O.; Roblegg, E.; Gruber-Woelfler, H.; Khinast, J. G. Continuous Sonocrystallization of Acetylsalicylic Acid (ASA): Control of Crystal Size. *Cryst. Growth Des.* **2012**, *12* (10), 4733−4738.
(51) Schmalenberg, M.; Weick, L. K.; Kockmann, N. Nucleation in Continuous Flow Cooling Sonocrystallization for Coiled Capillary Crystallizers. *J. Flow Chem.* **2021**, *11* (3), 303−319.
(52) Schmalenberg, M.; Kreis, S.; Weick, L. K.; Haas, C.; Sallamon, F.; Kockmann, N. Continuous Cooling Crystallization in a Coiled Flow Inverter Crystallizer Technology—Design, Characterization, and Hurdles. *Processes* **2021**, *9* (9), 1537.
(53) Jiang, M.; Papageorgiou, C. D.; Waetzig, J.; Hardy, A.; Langston, M.; Braatz, R. D. Indirect Ultrasonication in Continuous Slug-Flow Crystallization. *Cryst. Growth Des.* **2015**, *15* (5), 2486−2492.
(54) Jiang, M.; Zhu, Z.; Jimenez, E.; Papageorgiou, C. D.; Waetzig, J.; Hardy, A.; Langston, M.; Braatz, R. D. Continuous-Flow Tubular Crystallization in Slugs Spontaneously Induced by Hydrodynamics. *Cryst. Growth Des.* **2014**, *14* (2), 851−860.
(55) Vancleef, A.; Van Gerven, T.; Thomassen, L. C. J.; Braeken, L. Ultrasound in Continuous Tubular Crystallizers: Parameters Affecting the Nucleation Rate. *Crystals* **2021**, *11* (9), 1054.
(56) Vancleef, A.; De Beuckeleer, W.; Van Gerven, T.; Thomassen, L. C. J.; Braeken, L. Continuous Crystallization Using Ultrasound Assisted Nucleation, Cubic Cooling Profiles and Oscillatory Flow. *Processes* **2021**, *9* (12), 2268.
(57) Zhang, B.; Ådnebergli, I.; Stefanidis, G. D.; Van Gerven, T. Effects of Ultrasound on Reactive Crystallization and Particle Properties of an Aromatic Amine in Batch and Continuous Modes. *Ultrason. Sonochem.* **2024**, *111*, No. 107121.
(58) Roelands, C. P. M.; ter Horst, J. H.; Kramer, H. J. M.; Jansens, P. J. Precipitation Mechanism of Stable and Metastable Polymorphs of L-glutamic Acid. *AIChE J.* **2007**, *53* (2), 354−362.
(59) Vancleef, A.; Maes, D.; Van Gerven, T.; Thomassen, L. C. J.; Braeken, L. Flow-through Microscopy and Image Analysis for Crystallization Processes. *Chem. Eng. Sci.* **2022**, *248*, No. 117067.
(60) Gong, J.; Tang, W. Nucleation. In *Pharmaceutical Crystals*; Wiley, 2018; pp 47−88.
(61) Guo, Z.; Zhang, M.; Li, H.; Wang, J.; Kougoulos, E. Effect of Ultrasound on Anti-Solvent Crystallization Process. *J. Cryst. Growth* **2005**, *273* (3−4), 555−563.
(62) Hussain, M. N.; Jordens, J.; John, J. J.; Braeken, L.; Van Gerven, T. Enhancing Pharmaceutical Crystallization in a Flow Crystallizer with Ultrasound: Anti-Solvent Crystallization. *Ultrason. Sonochem.* **2019**, *59*, No. 104743.
(63) Hem, S. L. The Effect of Ultrasonic Vibrations on Crystallization Processes. *Ultrasonics* **1967**, *5* (4), 202−207.
(64) Devos, C.; Bampouli, A.; Brozzi, E.; Stefanidis, G. D.; Dusselier, M.; Van Gerven, T.; Kuhn, S. Ultrasound Mechanisms and Their Effect on Solid Synthesis and Processing: A Review. *Chem. Soc. Rev.* **2024**, DOI: 10.1039/D4CS00148F.
(65) Mawson, R.; Rout, M.; Ripoll, G.; Swiergon, P.; Singh, T.; Knoerzer, K.; Juliano, P. Production of Particulates from Transducer Erosion: Implications on Food Safety. *Ultrason. Sonochem.* **2014**, *21* (6), 2122−2130.
(66) Mendoza, H. R.; Pereira, M. V. L.; Van Gerven, T.; Lutz, C. Continuous Flow Synthesis of Zeolite FAU in an Oscillatory Baffled Reactor. *J. Adv. Manuf. Process.* **2020**, *2* (2), No. e10038.
(67) Lawton, S.; Steele, G.; Shering, P.; Zhao, L.; Laird, I.; Ni, X.-W. Continuous Crystallization of Pharmaceuticals Using a Continuous Oscillatory Baffled Crystallizer. *Org. Process Res. Dev.* **2009**, *13* (6), 1357−1363.
(68) Khan, S.; Ma, C. Y.; Mahmud, T.; Penchev, R. Y.; Roberts, K. J.; Morris, J.; Özkan, L.; White, G.; Grieve, B.; Hall, A.; Buser, P.; Gibson, N.; Keller, P.; Shuttleworth, P.; Price, C. J. In-Process Monitoring and Control of Supersaturation in Seeded Batch Cooling Crystallisation of L-Glutamic Acid: From Laboratory to Industrial Pilot Plant. *Org. Process Res. Dev.* **2011**, *15* (3), 540−555.

https://doi.org/10.1021/acs.oprd.4c00385
Org. Process Res. Dev. XXXX, XXX, XXX−XXX